

Direct-flux field-oriented control of IPM motor drives with robust exploitation of the Maximum Torque per Voltage speed range

Original

Direct-flux field-oriented control of IPM motor drives with robust exploitation of the Maximum Torque per Voltage speed range / Pellegrino, GIAN - MARIO LUIGI; Guglielmi, Paolo; Armando, Eric Giacomo. - STAMPA. - (2010), pp. 1-7. (2010 IEEE International Symposium on Industrial Electronics Bari (IT) 4-7 Luglio 2010) [10.1109/ISIE.2010.5637031].

Availability:

This version is available at: 11583/2376177 since:

Publisher:

IEEE

Published

DOI:10.1109/ISIE.2010.5637031

Terms of use:

This article is made available under terms and conditions as specified in the corresponding bibliographic description in the repository

Publisher copyright

(Article begins on next page)

Direct-flux field-oriented control of IPM motor drives with robust exploitation of the Maximum Torque per Voltage speed range.

Abstract—The direct-flux field oriented control of Interior Permanent Magnet motor drives is evaluated, with particular attention to very high speed operation in the maximum torque per voltage region. A new control technique is proposed to overcome the stability problem of direct flux control based on flux and quadrature current control. The proposed control is easy to be implemented, it is independent of the motor model, it is robust toward the effects of iron losses, of position estimation errors, of dc-link variations and inverter overmodulation. Experimental results are provided for a 600 W IPM drive for home appliances.

I. INTRODUCTION

Permanent magnet (PM) motors with flux weakening capability are appreciated for those applications where a constant power speed range (CPSR) is required, namely traction and spindle drives. A high CPSR can be obtained with different motor topologies, such as interior permanent magnet motors (IPM) or surface mounted PM motors with concentrated windings (SMPM) [1]. From a general point of view, independently of interior or surface mounted magnets, the flux weakening capability of such synchronous PM drives depends on the relationship between the motor characteristic current (1) and the drive rated current.

$$i_{ch} = \frac{\lambda_m}{L_d} \quad (1)$$

In particular, PM synchronous drives can be distinguished between finite and infinite speed range drives in case they have a rated current that is higher or lower than the characteristic current respectively [2]. The “infinite speed drives” respect the condition (2),

$$i_0 > i_{ch} \quad (2)$$

where i_0 is the drive rated current, that can be the motor rated current or more often the transient overload current of the motor. From the control point of view, the maximum power control strategy in flux weakening is generally based on the rotation of the current vector from its low speed, maximum torque per ampere position (MTPA) toward phase angles that augment the demagnetizing current component ($i_d < 0$). Such rotation reduces the motor linked flux and permits a higher speed at given inverter voltage, in the so called *current and voltage limited region* [2]. Moreover, with those PM drives that respect the condition (2), it is necessary to reduce the current amplitude above a certain speed according to the

maximum torque per voltage trajectory (MTPV) [3]. This is called the *voltage limited region*. The control trajectories of two example IPM drives are reported in Fig. 1: one with finite speed range and the other with infinite speed range. All the considerations in the following will be referred to salient IPM motor drives, but PM motor drives with isotropic rotors can be also controlled with the proposed control technique as will be explained in section IV.

The flux-weakening strategies of current-controlled IPM drives are based on control reference tables (i_d and i_q references) that require the identification of the motor model [4]. For tackling the variations of the motor parameters and the dc-link voltage, the closed-loop control of the motor voltage is also needed [5]. The stable control in the MTPV region requires proper techniques [6] but still current control remains sensitive to orientation errors (e.g. transducer alignment errors) and iron loss effects. In particular, for drives with high electrical frequency, the torque-current relationship must take into account the additional core loss current vector [7]. At very high speed the iron loss current is still smaller than the measured current, but the respect of the MTPV trajectory by means of current control becomes imprecise. Flux control is less sensitive to such effects [8].

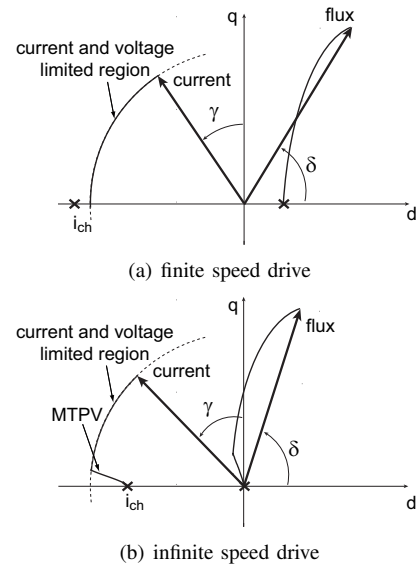


Fig. 1. Current and flux vector trajectories in flux weakening for finite-speed and infinite speed IPM motor drives.

Direct-flux field oriented control has been applied to IPM motors in [9], showing the following advantages:

- easy control of the motor voltage in flux weakening with no need for tables of current or flux references;
- easy adaptation to a variable dc-link with no firmware modification;
- direct limitation of the maximum motor current through the control of the quadrature current reference;
- low sensitivity to mechanical position estimation errors.

It must be noted that for the $\lambda - i_\tau$ control of [9], where i_τ is the quadrature or “torque” current component, the MTPV trajectory represents the boundary of the torque control stability region: crossing the MTPV path leads to the loss of control. In that work, the MTPV boundary was exploited by limiting the quadrature current according to a simplified motor model. The risk of instability has been avoided by setting such current limitation with a certain margin: in particular, the MTPV has been calculated in cold conditions that is with the maximum PM linked flux that is the worst case situation with the minimum size of the stable area of operation. Nevertheless that IPM motor drive, designed for traction, had a limited portion of the high speed range interested by the MPTV operation, thus the eventual loss of performance at high speed in hot conditions due to the MTPV margin was acceptable and difficult to be noticed: the base speed and maximum speed were 2450 rpm and 10000 rpm respectively, and the MTPV region was above 8500 rpm. In those motor drives with a higher current load and wider speed ranges, such as IPM drives for home appliances [10], the MTPV operation region interests a large portion of the operative speed range and the control margin can limit the delivered power at high speed with this direct flux control.

A proper control strategy is proposed to overcome such problem. The phase angle of the flux vector (δ , defined in Fig. 3) is limited to a maximum value δ_{max} that approximates the MTPV region and can be easily evaluated by experiments. The control of the maximum δ angle eliminates the instability toward the MTPV crossing: thus direct-flux field oriented control becomes easier to be implemented also for drives with a large MTPV speed range (2). The optimal limit angle δ_{max} can be found experimentally by ramping the motor to the maximum speed at no load of with an inertial load and seeking for the best acceleration performance with different δ_{max} trial values. Cold and hot PM conditions can be compared and a tradeoff can be found.

II. DIRECT-FLUX FIELD ORIENTED CONTROL

The direct-flux field oriented control technique presented in [9] is here briefly resumed with a more conventional choice of the reference axes. In [9] the dq rotor axes followed the PM-Assisted Synchronous Reluctance motor conventions, or 90-degrees ahead of the standard IPM notation. Moreover, the flux reference frame was called f, τ for indicating flux and torque. Here the IPM notation is adopted and the more comfortable names d_s, q_s are used for the stator flux oriented frame, like in stator flux field oriented control of IM drives. The rotor

and stator flux reference axes are defined in Fig. 3. Due to the different axes choice, some of the equations reported in this section are different with respect to [9]. In particular, equations (3-7) remain the same, while in equations (8-10) the terms L_d, L_q are exchanged and the terms with δ are 90 degrees shifted.

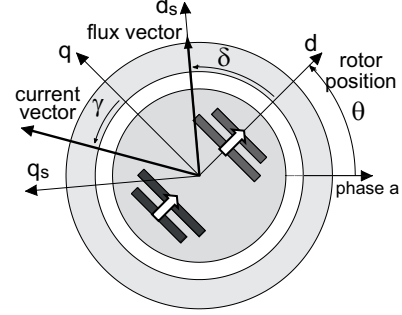


Fig. 3. Definition of dq rotor reference frame and d_s, q_s flux reference frame.

The simplified motor model of a salient PM motor is expressed in (3-5) in the rotor reference frame.

$$\bar{v}_{dq} = R\bar{i}_{dq} + \frac{d\bar{\lambda}_{dq}}{dt} + j\omega \cdot \bar{\lambda}_{dq} \quad (3)$$

$$\bar{\lambda}_{dq} = \begin{bmatrix} L_d & 0 \\ 0 & L_q \end{bmatrix} \cdot \bar{i}_{dq} + \begin{bmatrix} \lambda_m \\ 0 \end{bmatrix} \quad (4)$$

$$\frac{T}{3/2p} = \lambda_d i_q - \lambda_q i_d \quad (5)$$

Where p is the pole-pairs, R is the stator resistance, L_d, L_q are the dq inductances, λ_m is the PM flux, T is the electromagnetic torque. In the stator flux oriented frame the motor model becomes (6-7).

$$\bar{v}_{dqs} = R\bar{i}_{dqs} + \frac{d}{dt} \begin{bmatrix} \lambda \\ 0 \end{bmatrix} + \lambda \cdot \begin{bmatrix} 0 \\ \omega + \frac{d\delta}{dt} \end{bmatrix} \quad (6)$$

$$\frac{T}{3/2p} = \lambda \cdot i_{qs} \quad (7)$$

Where λ is the stator flux amplitude and δ is the phase angle with respect to the d rotor axis, defined in Fig. 3. In the voltage equation (6) the d_s and q_s equations are nearly decoupled (apart for the resistive term): the flux amplitude can be regulated by means of the v_{ds} component, while the flux phase angle can be regulated by v_{qs} . The resistive term in (6) is not decoupled since the dq_s current components both depend on λ and δ . The torque expression (7) is very simple and suggests the adoption of the torque-producing current i_{qs} on behalf of δ for achieving a straightforward control of the motor torque. For this reason, a further manipulation of (6) leads to the motor state equations in the controlled variables λ, i_{qs} [9].

$$\frac{d}{dt} \begin{bmatrix} \lambda \\ i_{qs} \end{bmatrix} \cong \begin{bmatrix} \frac{1}{k(\delta)} & 0 \\ \frac{b(\lambda, \delta)}{L_d} \end{bmatrix} \cdot \begin{bmatrix} v_{ds} \\ v_{qs} - \omega \lambda \end{bmatrix} \quad (8)$$

according to how accurately has the motor been identified. With the simplified motor model (4) and a motor with heavy cross-saturation, the control performance deteriorates a little bit at low speed, high load. However, even with a poor model, the phase current limit is still respected and the only possible drawback is the reduction of the controlled torque with respect to the torque set point. *Above the crossover frequency ($\omega > g$), the flux observer and thus the control are insensitive to the motor model and include the effect of core losses.*

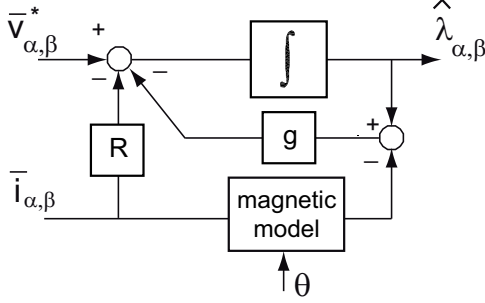


Fig. 4. Adopted flux observer.

C. Current and voltage limits

The motor phase current is limited to its rated value i_0 by limiting the q_s current reference according to (11).

$$i_{qs}^* \leq \sqrt{i_0^2 - i_{ds}^2} \quad (11)$$

The voltage limit is respected by limiting the linked flux according to the simplified flux-weakening law (12).

$$\lambda^* \leq \frac{V_{max} - R \cdot i_{qs}}{|\omega|} \quad (12)$$

where V_{max} is updated in real time according to the measured dc-link voltage for the full exploitation of the available voltage margin.

III. PROPOSED MTPV CONTROL STRATEGY

The IPM motor under test, whose ratings are reported in the Appendix, has been identified according to the procedure described in [13]: the dq flux model, complete of cross saturation, has been experimentally evaluated in the range $i_d = -5 \div 0A$, $i_q = 0 \div 5A$. According to the magnetic model, the control trajectories of Fig. 5 have been calculated in the current plane in dq rotor coordinates. The MTPA, i_0 and MTPV curves are represented in the figure and the characteristic current i_{ch} is nearly 2 A. The maximum power Vs speed profile has been also calculated (Fig. 6). The MTPV speed range is above the point called B in the figure, that is from 6500 rpm to 16000 rpm.

The same control trajectories can be calculated in the dq flux plane, in rotor coordinates, as done in Figs. 9 - 11. It can be noticed that in the flux plane the MTPV trajectory is well approximated by a line with constant δ angle. For the motor under test such angle is nearly $\delta = 126^\circ$. The tests

for the identification of the motor have been run at low speed (1500 rpm), thus the effects of iron losses are not considered in the theoretical control trajectories of Fig. 5 and 9, as will be shown in the next section.

The *MTPV current limitation* box in Fig. 2 consists of a PI regulator that corrects the q_s current limitation according to the phase angle of the observed flux with respect to the set point δ_{max} . Due to the relationship between the quadrature current i_{qs} and the flux phase δ , reducing i_{qs} leads to a corresponding reduction of δ . This means that in case δ tends to cross the δ_{max} limit, the i_{MTPV} terms arises and limits the q_s current to keep $\delta = \delta_{max}$. When the δ control is active, i.e. in torque saturation at high speed, the λ, i_{qs} control is practically replaced by a λ, δ control, that is stable toward the crossing of the MTPV line: in fact the δ derivative in (6) does not contain the b gain or other factors that change their sign around the MTPV locus. Apart for the PI gains tuning, that is not critical, the only condition to be respected is that the PI regulator output range must be large enough to keep the δ control, thus the upper limit of i_{MTPV} is set to the full current i_0 .

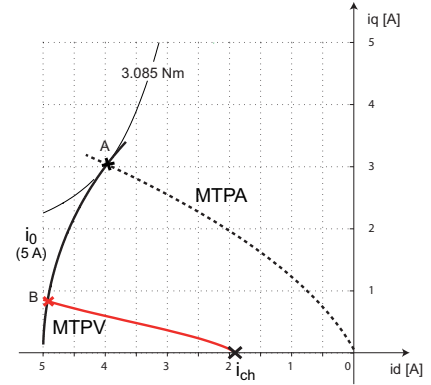


Fig. 5. Control trajectories in the dq current plane for the drive under test, according to the steady-state identification of the IPM motor.

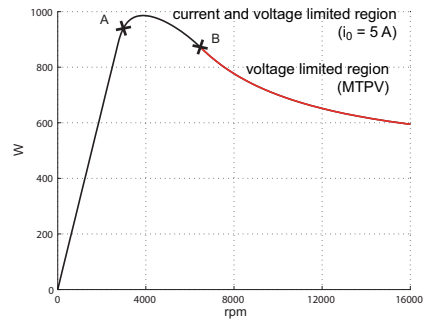


Fig. 6. Maximum power profile of the IPM motor drive under test, according to the steady-state identification of the IPM motor, with 5 A (pk) and 160 V (phase pk).

IV. EXPERIMENTAL RESULTS

A. Selection of the correct δ_{max}

A series of speed step tests is performed for evaluating the correct δ_{max} value, with the target of obtaining the fastest possible acceleration from zero to 16000 rpm. The step speed response is reported in Fig. 7 for three different δ_{max} values: 126° that is the value that best approximates the steady-state model of Fig. 9, 110° and 140° . The best speed dynamics is obtained with $\delta_{max} = 140^\circ$, while $\delta_{max} = 110^\circ$ is too margined and reduces the torque at high speed as expected. Thus, the actual maximum torque per voltage of the drive under test is over the theoretical path given by the steady-state model, as can be seen in Fig. 10. Such difference relies in the effect of iron losses, that modify the expression of torque with respect to (7) leading to modified control trajectories at high speed. The λ, i_{qs} control plots, referring to the $\delta_{max} = 126^\circ$ step of Fig. 7 are reported in Fig. 8, together with one phase current. The dynamic trajectories of the observed flux are reported for the three δ_{max} situations of Fig. 7 and compared to the theoretical control paths. The distortion of the flux trajectory is due to the inverter, since the overmodulation voltage region is exploited. Despite overmodulation, the $\delta = \delta_{max}$ operation is very smooth and regular, and the control is stable for any $\delta_{max} < 180^\circ$. Higher values up to $\delta_{max} = 170^\circ$ have been successfully tested with no stability problems and have not been reported due to space limitations. In case the controlled PM motor is a surface-mounted, isotropic motor, the same control concepts can be applied, with $\delta_{max} < 90^\circ$ [2].

B. Braking and motoring conditions

A speed reversal is shown in Fig. 12, and the related $\lambda, i_{qs}, i_{phase}$ plots are reported in Fig. 13. As expected, the deceleration phase is faster than the acceleration due to the effect of losses that contribute to brake the motor both in deceleration and acceleration. The flux amplitude reference is higher in braking (at the same speed) for a twofold reason: the resistive term in (12) that changes its sign and the higher dc-link voltage that augments the V_{max} value in (12). The dc-link voltage during the speed transient is reported in Fig. 14, showing the effect of brake resistance in deceleration and the 100 Hz ripple due to single-phase passive rectifier in acceleration.

V. CONCLUSIONS

The paper presents a solution for achieving a stable MTPV operation of IPM motor drives with direct flux field oriented control. The phase angle of the observed stator flux is controlled inside the proper operating region by means of a δ_{max} limiter block, based on a PI controller. With such limitation, the $\lambda - i_{qs}$ control is stable in all the speed range and the full torque capability of the motor is exploited up to very high speeds. The maximum torque per voltage trajectory can be found by experiments by comparing the motor acceleration with different δ_{max} values. The flux weakening control strategy is independent of the motor model and thus robust toward

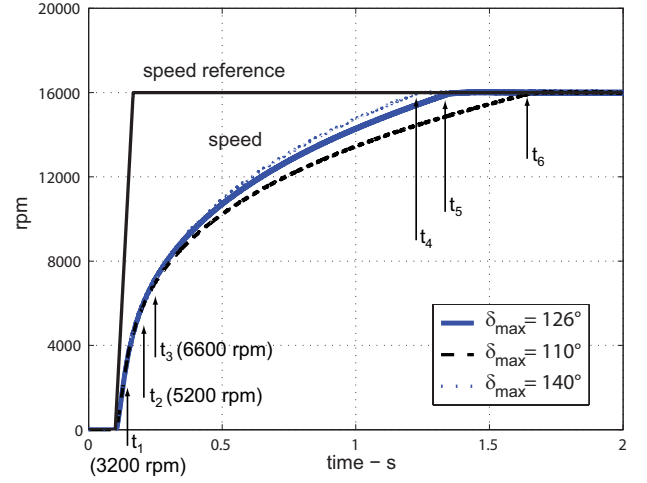


Fig. 7. Speed step response. Different δ_{max} values are evaluated, for selecting the one that leads to the maximum acceleration.

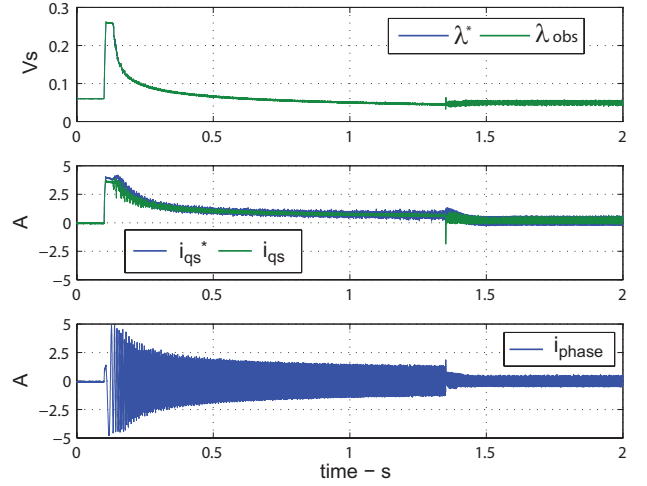


Fig. 8. Flux control, torque current control and phase current during the speed step transient of Fig. 7, with $\delta_{max} = 126^\circ$.

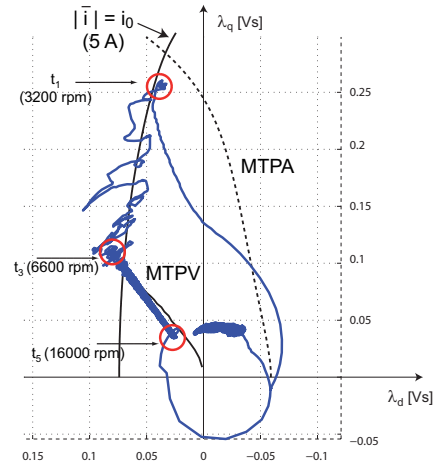


Fig. 9. $\delta_{max} = 126^\circ$: trajectory of the observed flux in the dq rotor frame during the speed step transient of Fig. 7.

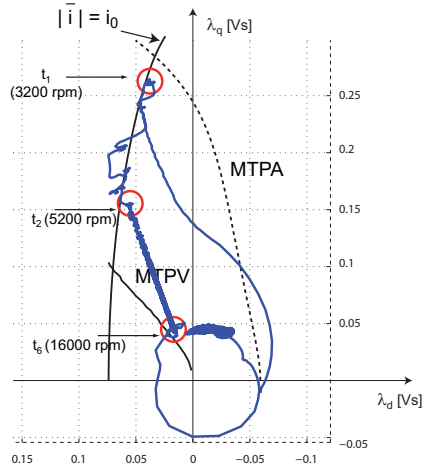


Fig. 10. $\delta_{max} = 140^\circ$: trajectory of the observed flux in the dq rotor frame during the speed step transient of Fig. 7.

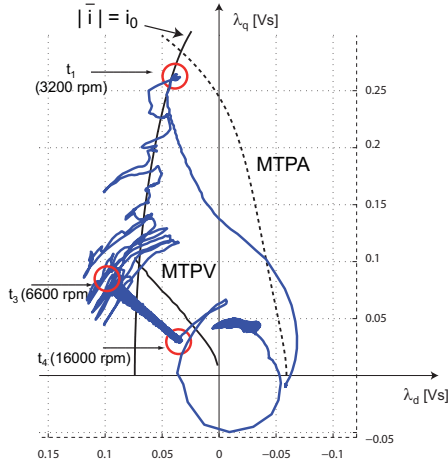


Fig. 11. $\delta_{max} = 110^\circ$: trajectory of the observed flux in the dq rotor frame during the speed step transient of Fig. 7.

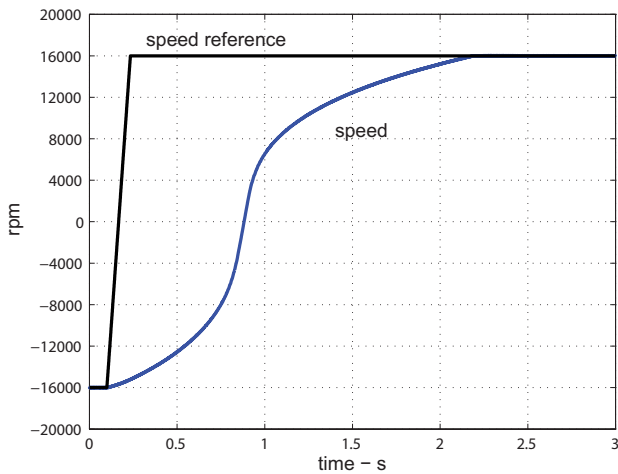


Fig. 12. Speed reversal response, $\delta_{max} = 126^\circ$.

parameter variations such as PM temperature variations. The full dc-link voltage is exploited also in case of variable dc-

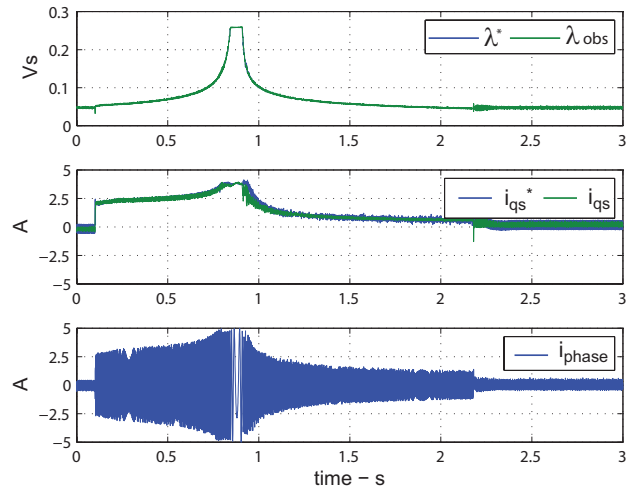


Fig. 13. Flux control, torque current control and phase current during the speed step reversal of Fig. 12.

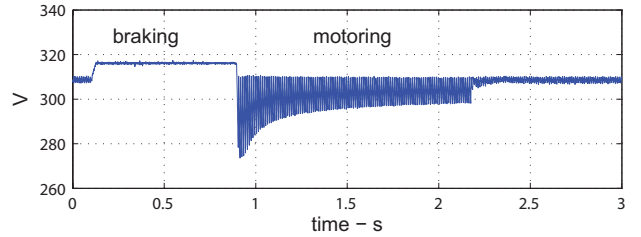


Fig. 14. Dc-link voltage during the speed step reversal of Fig. 12.

link and the maximum drive power is automatically exploited both in motoring and braking conditions with no firmware modification, also in presence of significant iron losses effects. Experimental tests demonstrate the feasibility of the proposed control.

APPENDIX: IPM DRIVE RATINGS

The motor under test is rated: 600 W, 160 V (phase, pk), 5 A (pk), 2 pole-pairs, 16000 rpm max. The inverter rating is: 220V, 50Hz single-phase input, passive rectifier with braking resistance. IGBT SOA: 600V, 10A. Dead-time setting is $1\mu s$. The switching frequency is 10kHz.

REFERENCES

- [1] A.M. EL-Refaie and T.M. Jahns. Comparison of synchronous pm machine types for wide constant-power speed operation: converter performance. *Electric Power Applications, IET*, 1(2):217–222, March 2007.
- [2] W.L. Soong and T.J.E. Miller. Field-weakening performance of brushless synchronous ac motor drives. *Electric Power Applications, IEE Proceedings* -, 141(6):331–340, Nov 1994.
- [3] S. Morimoto. Ipm vector control and flux weakening. In *TUTORIAL COURSE NOTES - Design, Analysis, and Control of Interior PM Synchronous Machines - IEEE Industry Applications Society Annual Meeting*, 2004.
- [4] S.Morimoto, Y.Takeda, T.Hirasa, and K.Taniguchi. Expansion of operating limits for permanent magnet motor by current vector control considering inverter capacity. *IEEE Transactions on Industry Applications*, 26(5):678–690, 1990.

- [5] J.Kim and S.Sul. Speed control of interior permanent magnet synchronous motor drive for the flux weakening operation. 33(1):43–48, 1997.
- [6] Bon-Ho Bae, N. Patel, S. Schulz, and Seung-Ki Sul. New field weakening technique for high saliency interior permanent magnet motor. In *Industry Applications Conference, 2003. 38th IAS Annual Meeting. Conference Record of the*, volume 2, pages 898–905 vol.2, Oct. 2003.
- [7] L. Xu, X. Xu, T.A. Lipo, and D.W. Novotny. Vector control of a synchronous reluctance motor including saturation and iron loss. *Industry Applications, IEEE Transactions on*, 27(5):977–985, Sep/Oct 1991.
- [8] A. Vagati, M. Pastorelli, and G. Franceschini. High-performance control of synchronous reluctance motors. *Industry Applications, IEEE Transactions on*, 33(4):983–991, Jul/Aug 1997.
- [9] G. Pellegrino, E. Armando, and P. Guglielmi. Direct flux field-oriented control of ipm drives with variable dc link in the field-weakening region. *Industry Applications, IEEE Transactions on*, 45(5):1619–1627, Sept.-oct. 2009.
- [10] E. Armando, P. Guglielmi, M. Pastorelli, G. Pellegrino, and A. Vagati. Performance of ipm-pmsr motors with ferrite injection for home appliance washing machine. In *Industry Applications Society Annual Meeting, 2008. IAS '08. IEEE*, pages 1–6, Oct. 2008.
- [11] Gubae Rang, Jaesang Lim, Kwanghee Nam, Hyung-Bin Ihm, and Ho-Gi Kim. A mtpa control scheme for an ipm synchronous motor considering magnet flux variation caused by temperature. In *Applied Power Electronics Conference and Exposition, 2004. APEC '04. Nineteenth Annual IEEE*, volume 3, pages 1617–1621 Vol.3, 2004.
- [12] N.Bianchi and S.Bolognani. Magnetic models of saturated interior permanent magnet motors based on finite element analysis. In *Proc. of IEEE Industry Applications Society Annual Meeting*, volume 1, pages 27 – 34, 1998.
- [13] A.Vagati, M.Pastorelli, F.Scapino, and G.Franceschini. Impact of cross saturation in synchronous reluctance motors of the transverse-laminated type. *IEEE Transactions on Industry Applications*, 36(4):1039 – 1046, 2000.